Components and targets of the PINOID signaling complex in Arabidopsis thaliana

Zago, Marcelo Kemel

Chapter 5

PINOID is a potential COP9 signalosome-associated kinase that modulates auxin response

Marcelo Kemel Zago, Felipe Maraschin, Rene Benjamins, Ab Quint, Remko Offringa

SUMMARY

The protein serine/threonine kinase PINOID (PID) is a signaling component in the control of polar auxin transport (PAT), as it determines the apico-basal polarity of the PIN family of auxin efflux carriers. The polar transport of auxin results in differential distribution of this hormone, and the cellular auxin concentrations are subsequently translated into a primary gene expression response. This last step occurs through the complex and cell-specific interactions between ARF transcription factors and labile Aux/IAA repressors. Abundance of Aux/IAA repressors is controlled by their auxin-induced, SCF^{TIR1} E3 Ligase-dependent proteolysis, a process that is regulated by the COP9 Signalosome (CSN).

We identified CSN subunit CSN8/COP9 as interacting partner of PID, and found that not CSN8, but the linked subunit CSN7/COP15, is phosphorylated by PID *in vitro*. PID overexpressing plants were observed to share constitutive photomorphogenic characteristics with *csn* down-regulated mutant lines suggesting that PID may be a repressor of CSN activity. An alternative role for PID as a putative CSN-associated kinase could be to regulate the interaction between E3 ligase and their proteolysis targets. To this point, we identified the labile auxin response repressor BODENLOS (BDL)/IAA12 as an *in vitro* phosphorylation target of PID. The observation that PID-mediated phosphorylation possibly occurs in the PRXS motif close to the SCF^{TIR1}-interacting domain II of BDL/IAA12 suggests that this event plays a role in the stability of this repressor protein. Analysis of the *pid-bdl* double mutant and transient expression experiments provided important *in vivo* data concerning the role of PID as a negative regulator of BDL activity during embryogenesis. Considering that BDL has a functionally redundant paralog IAA13, and that IAA13 also contains the PRXS motif, it is plausible that PID affects the activity of both AUX/IAAs. Whether PID controls the stability of BDL and IAA13 together or their interaction with ARF5/MP remains to be determined.

Although the mechanisms and roles of PID-mediated regulation of BDL, IAA13 or CSN require further elucidation, our data finally indicates that the PID protein kinase provides a direct link between auxin transport and -signaling.

Abbreviations: ARF, auxin response factor; AuxRe, auxin responsive element; AXR, auxin resistant; BDL/IAA12, Bodenloss/IAA12 protein; COP, constitutive photomorphogenesis; CSN, COP9 Signalosome; IAA, indole-3-acetic acid; MP, ARF5/Monopteros; NPH4, ARF7/Nonphotopropic hypocotyl 4; PAT, polar auxin transport; PID, pinoid; SCF, SKP1/Cullin/F-box

INTRODUCTION

The plant hormone auxin affects gene expression through the action of two types of transcriptional regulators: the auxin response factors (ARFs) and the Aux/IAA proteins. ARFs bind to promoters containing auxin responsive (AuxRE) elements and can either activate or repress transcription, depending on their domain structure (1). Aux/IAA proteins are short-lived nuclear proteins that function as repressors of auxin responsive gene expression. Most Aux/IAAs are encoded by auxin responsive genes themselves, and act in a feed-back loop to regulate their own expression (1). Aux/IAA proteins form a family of twenty-nine members in Arabidopsis that share four conserved domains (1). From amino- to carboxy-terminus, domain I has been shown to have transcription repression activity (2), domain II is involved in destabilization of Aux/IAA proteins, and may be target for ubiquitination (3), and domains III and IV have protein-protein interaction properties, allowing Aux/IAA proteins to homo- or heterodimerize with ARFs or other Aux/IAA proteins (4). The repression activity of Aux/IAA proteins is normally performed through their interaction with ARFs, that as a consequence can not dimerize to activate transcription (5). Several Arabidopsis *Aux/IAA* genes have been identified through gain-of-function mutations that stabilize the produced Aux/IAA protein. Usually, such gain-of-function mutations lead to reduced auxin response, as observed in the *bodenlos* (*bdl*) mutant, which apart from displaying auxin insensitivity lacks a primary root meristem and shows reduced hypocotyl growth and curled cotyledons (6). The phenotypes of *bdl* mutant seedlings imply that the BDL/IAA12 protein is involved in auxin-mediated apical-basal patterning of the Arabidopsis embryo.

In Arabidopsis, the stability of Aux/IAA proteins is regulated by the SCF^{TIR1} E3 Ubiquitin Ligase, a protein complex consisting of SKP1 (ASK1), CULLIN1 (CUL1), the RING protein RBX1 and the F-box protein TIR1 (7-9). High affinity binding of auxin to TIR1 was recently shown to enhance its affinity for Aux/IAA proteins, and to stimulate subsequent targeting of these proteins to the proteasome for degradation (10, 11). Mutants in components of this degradation pathway, such as *axr-1*, *tir-1* and *axr-6/cul1* were identified based on their impaired auxin response (7, 8, 12).

The activity of the SCF^{TIR1} E3 Ubiquitin Ligase is regulated by the COP9 Signalosome (CSN), a protein complex with homology to the lid of the 26S proteasome and an important regulator of photomorphogenesis in plants (13, 14). CSN interacts with the SCF^{TIR1} complex subunits CUL1 and RBX1 (15) and is involved in removal of RUB1, as part of the cyclic RUB modification of CUL1 that is essential for SCF activity (13, 16). Accordingly, mild loss-of-function mutants for the CSN5 subunit display phenotypes that are associated to defects in auxin response, and protein extracts from these plants do not degrade IAA6 from pea as efficiently as wild type plants extracts (15). More recently, it was shown that CSN, SCF^{TIR} and

26S proteasome components are recruited to nuclear bodies where Aux/IAA proteins are actively degraded (17). These findings place CSN, together with the proteolytic machinery, as a regulatory component of auxin signaling.

Apart from being translated into a primary gene expression response by the complex and cell-specific interaction of ARFs and Aux/IAA proteins, the auxin signal is primarily determined by its cellular concentration, which is again the result of biosynthesis and directional distribution through polar auxin transport (PAT). PAT-dependent differential distribution of auxin in young developing organs has been shown to be instrumental for a wide variety of developmental processes, such as embryogenesis (18), root development (19), shoot organogenesis (20), and tropisms (21-23). The chemiosmotic hypothesis proposed in 1970s suggested that the direction of PAT is determined by the polar subcellular localization of efflux carriers (24, 25). More recent molecular genetic studies with the model plant *Arabidopsis thaliana* have identified the PIN family of proteins to be essential for PAT. Analogous to the proposed efflux carriers in the chemiosmotic hypothesis, PIN proteins show auxin efflux activity and a polar subcellular localization that determines the direction of the auxin flow (18-21, 23, 26-31).

A substantial body of evidence from genetic and molecular approaches has determined that the serine/threonine kinase PINOID (PID) is a key component in the control of PAT. Recently, it was shown that the cellular levels of PID determine the apical-basal polarity of PINs. These observations explained the hypothesized changes in the auxin flow in PID loss and gain-of-function plant lines, implying that PID-mediated phosphorylation is essential for proper PAT and patterning processes (32, 33).

In addition to its central role as regulator of PAT, we identified two possible links between PID and auxin signaling. A screen for PID interacting proteins revealed that PID interacts with CSN8/COP9. *In vitro* phosphorylation assays indicated that PID does not phosphorylate CSN8/COP9, but instead phosphorylates CSN7/COP15, the subunit that is directly linked to CSN8/COP9 in the CSN complex (34). These results implicate that PID regulates the activity of the CSN. An alternative role for PID as a putative CSN-associated kinase could be to regulate the interaction between E3 ligase and their proteolysis targets. Moreover, we identified via *in vitro* assays that the labile auxin response repressor BODENLOS (BDL)/IAA12 is a phosphorylation target of PID. The observation that PID-mediated phosphorylation possibly occurs in the PRXS motif close to the SCF^{TIR1}-interacting domain II of BDL/IAA12 implicates that this changes the stability of this repressor protein. Intriguingly *pid-bdl* double mutants show an enhanced *pid* phenotype not present in either single mutant. Protoplast experiments provided further important indications for a role of PID as negative regulator of BDL. Together the data suggest that during embryogenesis PID inhibits specific IAA proteins that may include BDL/IAA12 and

IAA13, since IAA13 also has the potential phosphorylation site PRXS. The possible role of PID as modulator of auxin signaling will be discussed in light of its well-established role in directing PIN polar targeting.

MATERIALS AND METHODS

Molecular cloning and constructs

Molecular cloning was performed following standard procedures (35). The fusion GAL4BD (GAL4 Binding Domain)-PID was created as described by Benjamins (36). The construct GAL4AD (GAL4 Activation Domain)-COP9 was isolated from the yeast two-hybrid screen performed by Benjamins (36). The yeast two-hybrid bait plasmid pAS2-PBP2 was obtained by cloning a *PBP2 PstI/SalI*-blunted fragment derived from pSDM6014 into pAS2 digested with *PstI/XmaI*-blunted. The histidine tagged PID construct was created by excising the *PID* cDNA with *XmnI-SalI* from pSDM6005 (36) and cloning it into pET16H (pET16B derivative, J. Memelink, unpublished results) digested with *BamHI*, blunted and subsequently digested with *XhoI*. *CSN7* cDNA was amplified by PCR using the primers 5'-ACGCAAGTCGACAAGATGGATATCGAGCAGAAGCAAGC-3' and 5'- GATAGATCTAACAGAGGATCT TATACAAGTTG-3', and subsequently digested with *BglII* to be ligated into the pBluescriptSK+ plasmid treated with *EcoRV/BglII*. His-CSN7 was obtained by cloning *CSN7 BamHI/SalI* fragment into the plasmid pET16B (Novagen) digested with *XhoI/BamHI*. The construct encoding His-CSN8 was created by cloning *CSN8* fragment digested with *SalI* into pET16H treated with *XhoI/SmaI*. The preparation of the plasmids encoding His-PBP1 and GST-PID fusions have been described previously (37). The plasmid containing *35S::BDL* was obtained by cloning a partially digested *BDL NcoI/BamHI* fragment from pET16H-BDL into the pRT104 vector treated with the same enzymes. The *DR5::GUS* construct has been previously described (33). The *35S::PID* construct for protoplast transformation was generated as follows: initially the pEF-PID-FLAG plasmid was obtained, for which the overlapping oligos were designed: 3xFLAG#1 5'-GTACGCTTACTCCGCCGGAGATTCCTTCTTCCGTCGTCAAGAAGCCGATGAAAT-3', 3xFLAG#2 5'P-CGAAATGGATTATAAAGACCATGATGGAGATTAC-3', 3xFLAG#3 5'P-AAAGATCATGACATTGATTA TAAGGATGACGATGACATTGTCGACTGAC-3', 3xFLAG#4 5'-TCGAGTCAGTCGACAATGTCATCGTC ATCCTTATAATCAATGTC-3', 3xFLAG#5 5'-ATGATCTTTGTAATCTCCATCATGGTCTTTATAATCCA TTT-3' and 3xFLAG#6 5'-AACGTCGCCGATTTCATCGGCTTCTTGACGACGGAAGAAGGAATCTCCGG CGGAGTAAGC-3'. The oligos 3xFLAG#1 and #6, 3xFLAG#2 and #5 and 3xFLAG#3 and #4 were annealed and ligated to create the FLAG fragment. FLAG *BstWI/XhoI* fragment was subsequently cloned into pEF-PID (36) digested with the same enzymes. From the pEF-PID-FLAG plasmid, the PID-FLAG *EcoRI/XbaI* fragment was cloned into pART7 treated with the same enzymes.

Yeast two hybrid interaction

Using the Matchmaker II yeast two-hybrid system and *Saccharomyces cerevisiae* strain PJ69-4A (Clontech), COP9/CSN8 fused to the GAL4 activation domain (pACT2) was directly tested at 20^{o}C for interaction with PID or PBP2 fused to the GAL4 DNA binding domain (pAS2).

In vitro pull down experiments

GST tagged PID or GST protein alone were used in pull down assays with histidine (his)-tagged CSN8, BDL and PBP1 (H-proteins). Cultures of *E. coli* strain BL21 containing one of the constructs were grown at 37ºC to OD_{600} 0,8 in 50 ml LC supplemented with antibiotics. The cultures were then induced for 4 hours with 1 mM IPTG at 30ºC, after which cells were harvested by centrifugation (10 min. at 4.000 RPM in tabletop centrifuge) and frozen overnight at -20ºC. Precipitated cells were re-suspended in 2 ml Extraction Buffer (EB: 1x PBS, 2 mM EDTA, 2 mM DTT, supplemented with 0,1 mM of the protease inhibitors PMSF - Phenylmethanesulfonyl Fluoride, Leupeptin and Aprotinin, all obtained from Sigma) for

the GST-tagged proteins or in 2 ml Binding Buffer (BB: 50 mM Tris-HCl pH 6,8, 100 mM NaCl, 10 mM $CaCl_2$, supplemented with PMSF 0,1 mM, Leupeptin 0,1 mM and Aprotinin 0,1 mM) for the his-tagged proteins and sonicated for 2 min. on ice. From this point on, all steps were performed at 4ºC. Eppendorf tubes containing the sonicated cells were centrifugated at full speed (14.000 RPM) for 20 min., and the supernatants were transferred to fresh 2 ml tubes. H-proteins supernatants were left on ice, while 100 µl pre-equilibrated Glutathione Sepharose resin (pre-equilibration performed with three washes of 10 resin volumes of 1x PBS followed by three washes of 10 resin volumes of 1x BB at 500 RCF for 5 min.) was added to the GST- fusion protein containing supernatants. Resin-containing mixtures were incubated with gentle agitation for 1 hour, subsequently centrifugated at 500 RCF for 3 min. and the precipitated resin was washed 3 times with 20 resin volumes of EB. Next, all H-proteins supernatants (approximately 2 ml per protein) were added to GST-fusions-containing resins, and the mixtures were incubated with gentle agitation for 1 hour. After incubation, supernatants containing GST resins were centrifugated at 500 RCF for 3 min., the new supernatants were discarded and the resins subsequently washed 3 times with 20 resin volumes of EB. Protein loading buffer was added to the resin samples, followed by denaturation by 5 min. incubation at 95^0C. Proteins were subsequently separated on a 12% polyacrylamide gel prior to transfer to an Immobilon™-P PVDF (Sigma) membrane. Western blots were hybridized using a horse radish peroxidase (HRP)-conjugated anti-pentahistidine antibody (Quiagen) and detection followed the protocol described for the Phototope-HRP Western Blot Detection Kit (New England Biolabs).

In vitro phosphorylation assays

All proteins used in *in vitro* phosphorylation assays were his-tagged for purification from several (usually five) aliquots of 50 ml cultures of *E. coli*. strain BL21 which were grown, induced, pelleted and frozen as described above for the *in vitro* pull down experiments. Each aliquot of frozen cells pellet was resuspended in 2 ml Lysis Buffer (25 mM Tris-HCl pH 8,0; 500 mM NaCl; 20 mM Imidazol; 0,1% Tween-20; supplemented with 0,1 mM of the protease inhibitors PMSF, Leupeptin and Aprotinin) and subsequently sonicated for 2 min. on ice. From this point on, all steps were performed at 4ºC. Sonicated cells were centrifugated at full speed (14.000 RPM) for 20 min, the new pellets were discarded, and supernatants from all aliquots of the same construct were transferred to a 15 ml tube containing 100 µl of pre-equilibrated Ni-NTA resin (pre-equilibration performed with three washes of 10 resin volumes of Lysis Buffer at 500 RCF for 5 min.). Supernatant and resin were incubated with gentle agitation for 1 hour. After incubation, supernatant containing Ni-NTA resin was centrifuged at 500 RCF for 3 min., the new supernatant was discarded and the resin subsequently washed: 3 times with 20 resin volumes of Lysis Buffer, once with 20 resin volumes of Wash Buffer 1 (25 mM Tris.Cl pH 8,0; 500 mM NaCl; 40 mM Imidazol; 0,05% Tween-20) and once with 20 resin volumes of Wash Buffer 2 (25 mM Tris-HCl pH 8,0; 600 mM NaCl; 80 mM Imidazol). In between the washes, the resin was centrifugated for 5 min. at 500 RCF. After the washing steps, 20 resin volumes of Elution Buffer (25 mM Tris.HCl pH 8,0; 500 mM NaCl; 500 mM Imidazol) was added to the resin and incubated for 15 min. with gentle agitation. The resin was centrifugated for 3 min. at 500 RCF, and the supernatant containing the desired protein was diluted a 1000-fold in Tris Buffer (25 mM Tris.HCl pH7,5; 1 mM DTT) and concentrated to a workable volume (usually 50 µl) using Vivaspin microconcentrators (10 kDa cut off, maximum capacity 600 µl, manufacturer: Vivascience). Glycerol was added as preservative to a final concentration of 10% and samples were stored at -80ºC.

Approximately 1 µg of each purified his-tag protein (PID and substrates) in maximal volumes of 10 µl were added to 20 µl kinase reaction mix, containing 1x kinase buffer (25 mM Tris-HCl pH 7,5; 1 mM DTT; 5 mM $MgCl_2$) and 1 x ATP solution (100 µM $MgCl_2$/ATP; 1 µCi ^{32}P-γ-ATP). Reactions were incubated at 30ºC for 30 min. and stopped by the addition of 5 µl of 5 x protein loading buffer (310 mM Tris-HCl pH 6.8; 10 % SDS; 50% Glycerol; 750 mM β-Mercaptoethanol; 0,125% Bromophenol Blue) and 5 min. boiling. Reactions were subsequently separated over 12,5% acrylamide gels, which were washed 3 times for 30 min. with kinase gel wash buffer (5% TCA – Trichoroacetic Acid; 1% $Na_2H_2P_2O_7$), coomassie stained, destained, dried and exposed to X-ray films for 24 to 48 hours at -80ºC using intensifier screens.

For the peptides assays, 1µg of purified PID was incubated with 4 nmol of 9^{mer} biotinilated peptides (Pepscan) in a phosphorylation reaction as described above. Reaction processing, spotting and washing of the SAM^2 Biotin Capture Membrane (Promega) were performed as described in the corresponding protocol. Following washing, the membranes were wrapped in plastic film and exposed to X-ray films for 24 to 48 hours at -80^{o}C using intensifier screens. The phosphorylation intensities of each peptide were determined by densitometry analysis of the autoradiographs using the ImageQuant software (Molecular Dynamics).

Protoplast transformations

Protoplasts were obtained from *Arabidopsis thaliana* Col-0 cell suspension cultures that were propagated as described by Schirawski and co-workers (38). Protoplast isolation and PEG-mediated transformation followed the protocol described originally by Axelos and co-workers (39) and adapted by Schirawski and co-workers (38). The transformations were performed with 10 µg of the constructs *DR5::GUS* and *35S::PID,* 1 µg of *35S::BDL*, and 2 µg of a plasmid expressing Renilla luciferase for signal normalization, after which the protoplasts were incubated for at least 16h. Subsequent treatments of the prepared protoplasts employed IAA 1 µM for a period of 8 hours.

Plant growth

Seeds were germinated and seedlings grown *in vitro* on MA medium (40) supplemented with antibiotics or other compounds when required, at 21^{o}C, 50% relative humidity and a 16 hours photoperiod of 2500 lux. Flowering Arabidopsis plants were grown on substrate soil, in growth rooms at 20^{o}C, 40% relative humidity and a 16 hours photoperiod of 2500 lux.

RESULTS

PINOID interacts with CSN8/COP9 and phosphorylates CSN7/COP15 *in vitro*

One of the PID interacting proteins identified using the yeast two-hybrid system (36) was the subunit 8 of the CSN (CSN8/COP9). This interaction was confirmed by re-transformation of the respective bait and prey vectors into the yeast strain PJ69-4A (Figure 1A) and by *in vitro* protein pull-down assays (Figure 1B).

Only few kinases have been shown to associate with the CSN. For example, Uhle and co-workers (41) demonstrated that the proteins CK2 and PKD bind CSN Subunit 3 and phosphorylate CSN Subunits 2, 5 and 7. Based on this information, we hypothesized that PID phosphorylates CSN8/COP9 or another subunit of the CSN complex. Our initial *in vitro* phosphorylation assays did not show any evidence that PID phosphorylates CSN8/COP9 (Figure 1C). Since it has been shown that CSN8/COP9 interacts with the phosphoprotein CSN7 (34, 41, 42), we directly tested if CSN7 could be phosphorylated by PID *in vitro*. Indeed, CSN7 was efficiently phosphorylated by PID and in our assays CSN7 phosphorylation occurred independently of CSN8/COP9 (Figure 1C). Most likely the excess of PID and CSN7 used in these experiments overruled the requirement for CSN8/COP9-mediated PID anchoring.

The NetPhos program (43) was used to identify putative amino acids in CSN7 that are targets for PID phosphorylation, and this *in silico* analysis identified eight potential CSN7 phosphorylation sites (Figure 1D). To test each of these residues we synthesized eight biotinylated peptides, only six of which could be used in phosphorylation reactions as the other two were insoluble (Figure 1E). The two peptides with the amino acid sequence core KRASTCKS, which starts at position 16 in the CSN7 protein, were most efficiently phosphorylated by PID (Figure 1E). More detailed analysis of these peptides in the ScanProsite database (44) indicated that they share characteristics of phosphorylation substrates of cyclic AMP dependent Protein Kinase (PKA: R/K-R/K-X-S/T) and of Protein Kinase C (PKC: S/T-X-R/K). Pep-Chip experiments have shown that PID efficiently phosphorylates PKA and PKC substrates (Galvan-Ampudia and Offringa, unpublished data), therefore either CSN7 serine 19 or threonine 20 are interesting putative PID phosphorylation targets. These results suggest that PID possibly regulates CSN activity through phosphorylation of subunit CSN7.

35S::PID lines show weak constitutive photomorphogenesis

The possible role of PID as regulator of the CSN, and the fact that the CSN complex has been discovered as repressor of photomorphogenesis (45), suggested that plant lines with altered *PID* expression may develop photomorphogenesis-related seedling phenotypes. The fact that no such phenotypes were observed in *pid* mutant seedlings may be explained by the specific role of PID in organogenesis in the embryo and inflorescence (33, 46, 47) and that other related kinases may be functionally redundant with PID. The mutant phenotypes of the *35S::PID* gain-of-function lines, however, are strongest in the seedling stage. Several of the strong auxin related features such as the collapse of the main root meristem and agravitropic growth are well-accounted for by the changes in PIN polar targeting (32, 33). However, *35S::PID* plants show a delay in lateral root formation, a phenotype that is also observed in *csn5* reduction-of-function lines (15). Furthermore, *35S::PID* seedlings present mild constitutive photomorphogenic characteristics that are observed in the *cop/fus* mutants (14). These phenotypes include lack of an apical hook and opening of cotyledons when grown in the dark and enhanced accumulation of anthocyanins when grown under light are also observed in *35S::PID* (Figure 2). Although these observations suggest that the role of PID as CSN-associated kinase is to repress CSN activity, further *in vivo* studies are required to clarify the functional relationship between PID and the CSN.

bodenlos is an enhancer of *pinoid*

The CSN has been shown to regulate proteolysis of AUX/IAA proteins through its interaction with the SCF^{TIR} E3 ligase (13, 15, 17, 48). The interaction of PID with

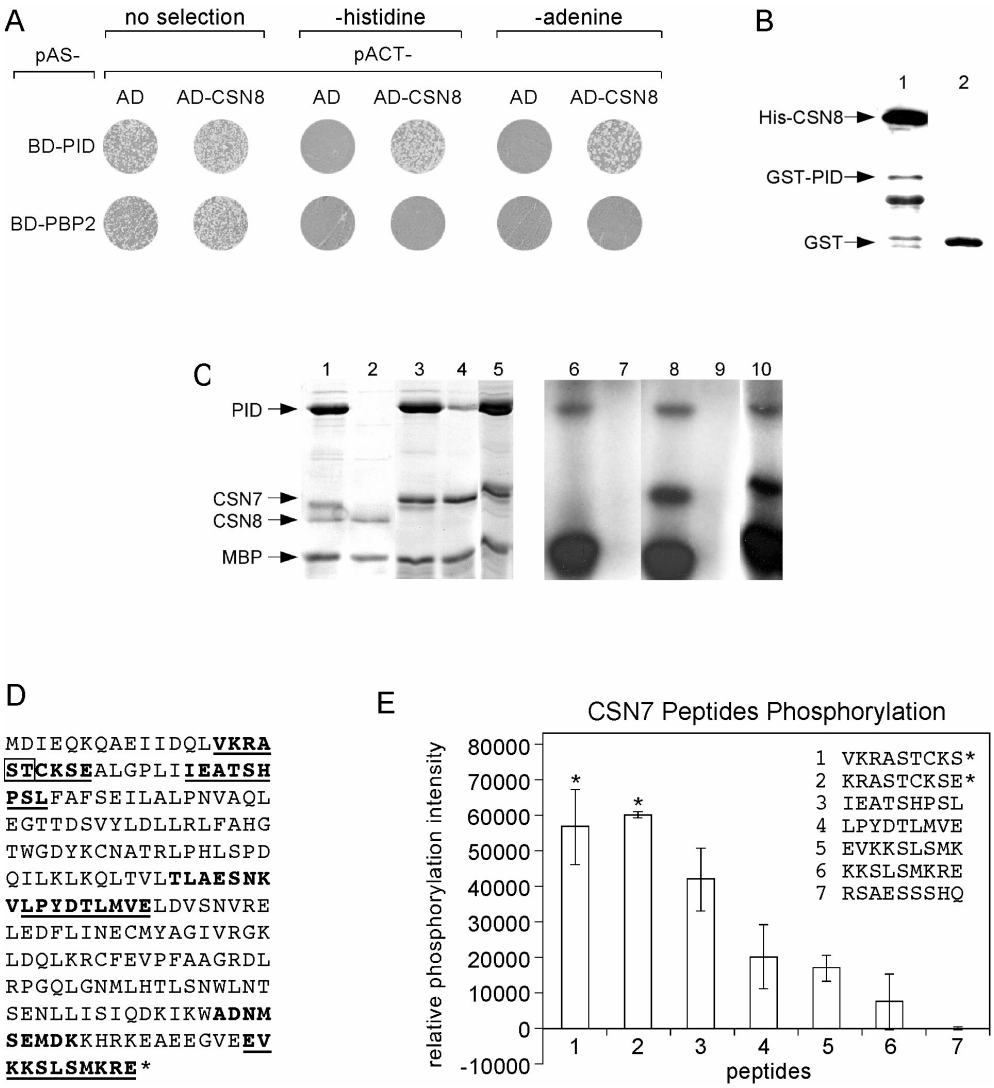

Figure 1. PID interacts with CSN8/COP9 and phosphorylates CSN7/COP15. (A) Yeast two-hybrid assay with PID and PBP2 fused to the GAL4 DNA binding domain (BD; pAS vector), and CSN8/COP9 fused to the GAL4 activation domain (AD) or the AD alone (pACT vector) in non-selective medium or in medium lacking either histidine or adenine. (B) *In vitro* pull-down of his-tagged CSN8/COP9 with GST-tagged PID (lane 1) and not with GST (lane 2), as shown by immunodetection with anti-his antibodies (top panel). The comassie stained gel is shown in the bottom panel. (C) Autoradiograph (right panel) and coomassie stained gel (left panel) of *in vitro* phosphorylation assay using MBP (all lanes), his-CSN8 (lanes 1, 2, 5, 6, 7 and 10) and his-CSN7 (lanes 3, 4, 5, 8, 9 and 10) as substrates and PID (lanes 1, 3, 5, 6, 8 and 10) as protein kinase. (D) Amino acid sequence of CSN7, with the eight putative phosphorylation sites identified by NetPhos (Blom *et al.*, 1999) as central residues within nine aminoacids peptides indicated in bold. The peptides tested in the *in vitro* phosphorylation assay (E) are underlined and the putative PID phosphorylation substrates are boxed in (D). BDL peptide RSAESSSHQ (7) was used as a negative control.

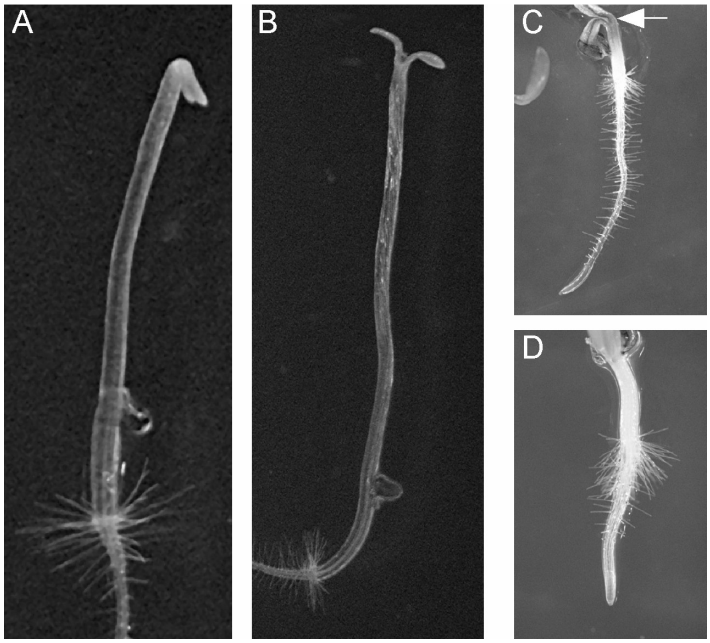

Figure 2. PID overexpression plants display mild constitutive photomorphogenic characteristics. Three-day-old seedlings of Columbia WT (A and D) and *35S::PID* (B and C) grown in dark (A and B) and light (C and D). The area in the upper-hypocotyl with high accumulation of anthocyanin in a *35S::PID* seedling is indicated with an arrow (C).

CSN entertained the possibility that PID may be involved in regulating the stability of Aux/IAA proteins (5). Since PID is expressed in the embryo and is essential for proper embryonic patterning (33, 46, 49), we decided to test whether PID could alter the activity of the embryonic Aux/IAA protein BODENLOS (BDL)/IAA12.

A *pid* loss-of-function mutant allele was crossed with the *bdl* gain-of-function mutant. F2 seedlings from this cross displayed a range of phenotypes, varying from wild type and typical *pid* and *bdl* seedlings to seedlings that lack or only develop rudimentary cotyledons (no-cot), or no-cot seedlings that even lack a primary root (Figure 3A to 3D). As the latter seedlings phenocopied the previously identified *gurke* mutants (50), their phenotype was referred to as *gurke*-like. The frequency of no-cot or *gurke*-like seedlings matched the expected numbers for respectively *BDL*/*bdl pid*/*pid* and *bdl*/*bdl pid*/*pid* progeny (Table 1). Few seedlings of the no-cot and *gurke*-like class were able to grow beyond the seedling stage, but showed a completely disorganized phyllotaxis and formed early pin-like inflorescences (Figure 3E). The no-cot phenotype was also observed in *pid-pin1* double mutants (49), and since we know now that PID regulates PIN polar targeting (32), these results suggest that a functional interaction may also exist between PID and BDL.

PID reduces BDL-mediated repression of auxin responsive gene expression

Considering the possible effect of PID on BDL action, we decided to test whether this interaction could be directly observed on the gene expression level in Arabidopsis protoplasts. In this system, expression of the auxin responsive *DR5::GUS* reporter gene was significantly induced by 8 hours treatment with 1 µM IAA. Co-transformation of the *DR5::GUS* reporter with the *35S::BDL* construct resulted in a 50% reduction of the IAA-induced reporter gene activity (Figure 3F). When the *DR5::GUS* and *35S::BDL* constructs were co-introduced together with the *35S::PID* plasmid, auxin-induced GUS expression was restored to approximately 90% of the activity in the control transformation with the reporter gene alone (Figure 3F). The *35S::PID* construct itself did not significantly alter *DR5::GUS* activity (Figure 3F). In these assays the amount of plasmid DNA transformed for each construct was variable, meaning that the different transformed protoplast samples contained different amounts of total plasmid. Therefore, we cannot fully exclude that this influenced the data obtained. In spite of this, our results appear to indicate that PID can antagonize the repression of auxin responsive gene expression by BDL. Together with the observed synergistic phenotypes in the *pid-bdl* double mutants, these results suggest that PID activity represses BDL.

PID phosphorylates, but does not interact directly with BDL *in vitro*

To find more evidence for the putative functional interaction between PID and BDL, we tested whether PID phosphorylates or binds to BDL *in vitro*. Although we did not observe a clear interaction between the two proteins in pull down assays (Figure 4A), we did detect a strong PID-dependent phosphorylation of BDL (Figure 4B).

By using the NetPhos software (43), thirteen putative phosphorylation sites were mapped in the BDL protein (Figure 4C). Biotinylated peptides corresponding to these sites were synthesized and ten soluble peptides were used in *in vitro* phosphorylation reactions. The peptides with the amino acid sequences MRGVSELEV (Peptide 1), PPRSSQVVG (Peptide 5) and LKDVSMKVN (Peptide 6) in BDL were strongly phosphorylated by PID (Figure 4D), and phosphorylation of peptide 9 was rather variable. Further analysis of the amino acid sequences of the consistently phosphorylated peptides by the ScanProsite (44) and NetPhos software (43) indicated that Peptide 1 comprises the phosphorylation consensus of Casein Kinase 2 (CK2: S/T-X-X-D/E), Peptide 5 contains the consensus of DNA-Dependent Protein Kinase (DNAPK: S/T-Q) and Peptide 6 shows the consensus of Protein Kinase C (PKC: S/T-X-R/K). Interestingly, peptide 5 comprises the PRXS motif that was also present in the two major PID target sites identified in PIN1 (Figure 4E and Chapter 4). The fact that the serine residue of this motif is located close to the

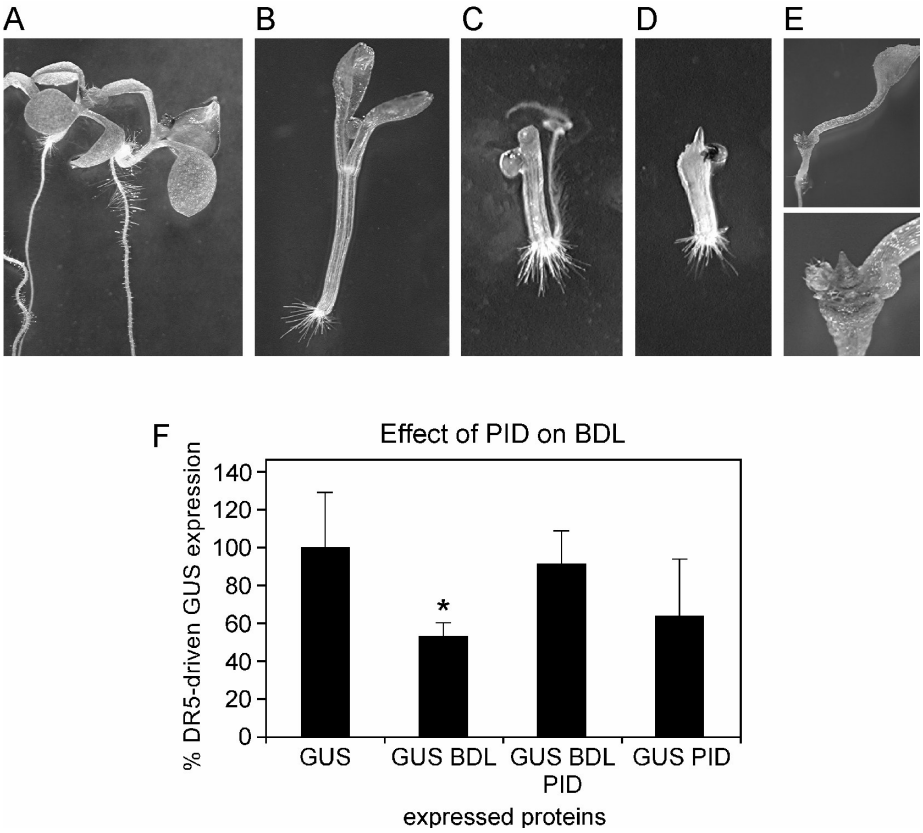

Figure 3. PID antagonizes the transcriptional repressor activity of BDL. The *bdl* gain-of-function mutation enhances the cotyledon defects of the *pid* loss-of-function mutant (A-E). The phenotypes of the *pid* (A) and *bdl* (B) parental lines and the synergistic no-cot (C) and *gurke*-like (D) phenotypes observed in the *pid* x *bdl* F2 population. Older no-cot and *gurke*-like seedlings display disorganized phyllotactic pattern and early formation of pin structures (E). (F) Auxin-induced *DR5::GUS* expression in Arabidopsis cell suspension-derived protoplasts is repressed by *35S::BDL* and this repression is alleviated by co-transformation of *35S::PID*. Co-transformation of *35S::PID* alone does not significantly affect *DR5::GUS* activity. The protoplasts were treated for 8 hours with 1 µM IAA. The star indicates a significant difference with the *DR5::GUS* control transformation using Student's t-test (t=3,75; p>0,05; 7 GUS and 6 GUS BDL samples were analyzed).

conserved part of domain II makes it tempting to speculate that PID-mediated phosphorylation at this specific position enhances the SCF^{TIR1}-dependent proteolysis of BDL.

An alignment of 27 Arabidopsis Aux/IAA proteins showed that, although several other Aux/IAAs have a serine or threonine at the same domain II-linked position, the PRXS motif is only found in IAA12/BDL and IAA13 (Figure 4E). This, together with the recently identified functional redundancy between IAA12/BDL and IAA13 (51),

suggests that PID controls the proteolysis of both proteins during embryo development. The synergistic phenotypes observed in *bdl-pid* double mutants could be explained by the enhanced IAA13 stability as a consequence of the absence of PID regulatory activity during cotyledon development.

Table 1. Segregation analysis of phenotypes observed in a *pid* x *bdl* F2 population

		Phenotypic classes				
	Total	kans ξ	tricot†,*	*bdl**	no-cot.*	*gurke*-l*
Observed number of seedlings (%)	198 (100)	50 (25)	6 (3)	17 (8,5)	13 (6)	4 (2)
Expected number of seedlings (%)	198 (100)	50 (25)	6 (3)	25 (12,5)	12 (6)	6 (3)

ξ Seedlings homozygous for the wild type *PID* gene and kanamycin sensitive, as seeds were germinated on MA medium containing 25µg/ml of kanamycin, to select for the T-DNA insertion causing the *pid* loss-of-function mutation.
† The three cotyledon phenotype of this *pid* mutant allele shows a penetrance of 50%, indicating that it is a complete loss-of-function allele (Bennett *et al.,* 1995; Christensen *et al.*, 2000).
*The expected number of kanamycin resistant three cotyledon, *bdl*, no-cotyledon and "*gurke*-like" seedlings, based on 1:16 (*BDL/BDL pid/pid*), 1:8 (*bdl/bdl PID/pid*), 1:8 (*BDL/bdl pid/pid*) and 1:16 (*bdl/bdl pid/pid*) segregation ratios, respectively, and a 50% penetrance of the phenotypic changes induced by the homozygote *pid* mutation. The numbers between brackets indicate percentages. The observed numbers did not significantly differ from the expected ones in the X^2 test (X^2=3,69, p<0,05).

DISCUSSION

Several lines of evidence indicate that at several steps auxin controls its own polar transport. For example, auxin was found to inhibit the endocytosis step in the cyclic trafficking of PIN vesicles between PM and endosomal compartments, thereby increasing the levels of PM localized PINs to promote its own efflux (52). In gravistimulated roots, the redistributed auxin was shown to affect both PIN2 localization and protein levels (53). Moreover, the directionality of PAT is regulated by the PID protein kinase that controls the polar subcellular localization of the PIN auxin efflux carriers (32). The observation that auxin controls cellular PID levels (33), suggests that PID is involved in a feedback mechanism by which auxin directs its own efflux. Overall, the three observations suggest that auxin signaling and -transport processes are tightly linked by regulatory feedback loops.
In this chapter we present preliminary data suggesting that the PID protein kinase, next to its auxin-enhanced cellular levels, also provides a direct link between auxin transport and -signaling. Firstly, we obtained evidence that PID interacts with and phosphorylates the CSN, a central component in E3-ligase-dependent degradation of proteins such as the Aux/IAA repressors of auxin responsive gene expression. Secondly, our results suggest that PID antagonizes the action of IAA12/BDL and

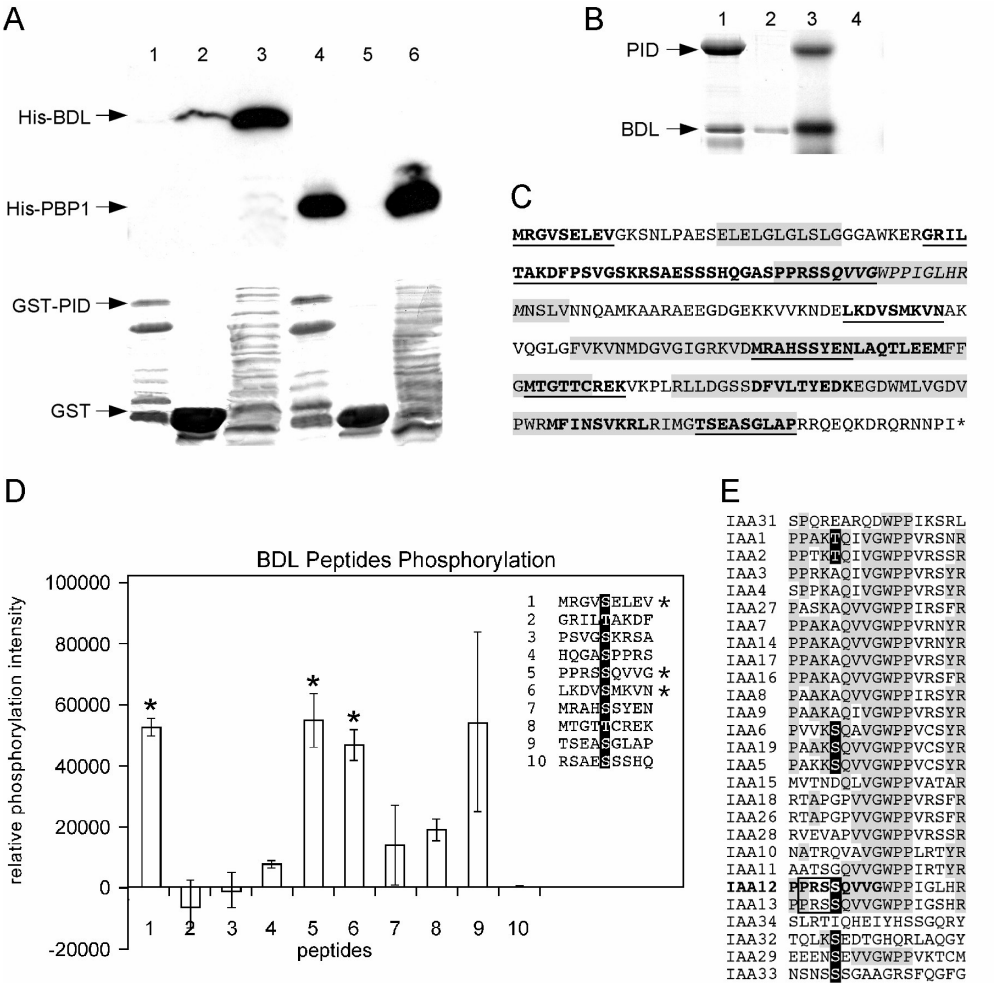

Figure 4. PID does not interact with, but phosphorylates BDL. (A) An *in vitro* protein pull-down assay showing that his-tagged BDL (lanes 1 to 3) is not pulled down with GST-PID (lane 1) nor with GST alone (lane 2), whereas his-tagged PBP1 (lanes 4 to 6) is specifically pulled down with GST-tagged PID (lane 4) and not with GST alone (lane 5). Total protein extracts (1% of input) of *E. coli* cells expressing his-BDL (lane 3) or his-PBP1 (lane 6) are loaded as controls. The top panel shows immunodetection of his-tagged proteins, and the coomassie stained gel is shown in the bottom panel. (B) Coomassie stained gel (lanes 1 and 2) and autoradiograph (lanes 3 and 4) of an *in vitro* phosphorylation reaction with PID (lanes 1 and 3) and BDL (all lanes). (C) BDL protein sequence with domains I, II, III and IV shaded, all putative phosphorylation residues identified by NetPhos (Blom *et al.*, 1999) within nine aminoacids peptides indicated in bold, and the peptides used in *in vitro* phosphorylation assays underlined. The highly conserved portion of domain II is in italics. (D) Relative radioactive labeling intensities of different BDL-derived peptides by PID in *in vitro* phosphorylation reactions. The BDL-derived peptides that are highly phosphorylated by PID are indicated with a star. (E) Alignment of the conserved part of domain II of 27 Arabidopsis Aux/IAAs. Gray shading shows conserved residues. Putative phosphorylation sites at position 5 are shaded in black and the PRXS motif that is unique for BDL/IAA12 and IAA13 is boxed.

IAA13 during embryogenesis as a direct result of phosphorylation on these repressors at a site close to the conserved domain II. Below we will discuss the implications of our findings, which are rather surprising in light of the well-established role of PID in directing the subcellular trafficking of PIN proteins.

PID as a possible CSN-associated kinase

Our observations provide the first clues that a plant protein kinase is associated with the CSN. CSN-associated kinases have been identified in bovine and human cells; inositol 1,3,4 triphosphate 5/6 kinase was shown to physically interact with CSN subunit CSN1 (54), and the kinases CK2 and PKD were shown to interact with CSN subunit CSN3 and to phosphorylate CSN2, CSN5 and CSN7 (41). The three CSN-associated kinases were also shown to phosphorylate and thereby control the stability of the regulatory proteins p53 and c-JUN (41, 54-56).

The role of PID as CSN-associated kinase is as yet unclear. *35S::PID* seedlings phenocopy some of the constitutive photomorphogenesis aspects of *csn* down-regulated mutants or lines overexpressing the photomorphogenesis promoting transcription factor HY5, a target of the CSN-dependent COP1 E3 ligase (15, 57, 58). This suggests that PID acts as a negative regulator of CSN activity. Interestingly, HY5 phosphorylation at a CK2 consensus site in the COP1 interacting domain was shown to lower the affinity for COP1 and to stabilize this transcription factor (58). It seems most likely, however, that HY5 phosphorylation is not performed by PID, but by the plant CK2 that is possibly associated with CSN, and that has been implied in promoting light regulated plant growth in Arabidopsis (59).

What would then be the role of PID in association with CSN? PID could regulate the stability of other targets of the CSN-E3 ligase proteolysis pathway. This second hypothesis is supported by our observation that the CSN-SCF^{TIR1} E3 ligase target IAA12/BDL is phosphorylated by PID *in vitro*. The alternative role of PID as CSN-associated kinase could be to regulate the activity or stability of the CSN complex itself by phosphorylating CSN7. To test this option, we would have to reevaluate the putative PID phosphorylation sites through site directed mutagenesis of CSN7 and subsequent testing of the mutant forms in *in vitro* phosphorylation assays. Based on the conclusive identification of the amino acids phosphorylated by PID, mutant forms of CSN7 that miss the phosphorylation site or that mimic constitutive phosphorylation should then be expressed in a *csn7* loss-of-function mutant back ground, to identify the *in vivo* significance of PID-mediated phosphorylation of CSN7.

The role of PID as CSN-associated kinase could also relate to its function in directing the polar subcellular targeting of PIN proteins. Previously, we have shown that enhanced cellular PID levels can redirect PIN proteins from a basal (bottom) to an apical (top) subcellular localization within a 12 to 16 hours time frame (32). This

polarity switch could involve proteolytic degradation of the basally localized PIN1 proteins, and PID-mediated phosphorylation of PINs (see Chapter 4 of this thesis) could enhance the affinity of these proteins for the corresponding E3-ligase. In yeast and mammalian cells, ubiquitination of membrane proteins, a step that is often preceded by phosphorylation, provides a key signal for endosomal sorting of membrane proteins (60). Interestingly, for PIN2 it has recently been shown that cellular levels and intracellular relocation of this protein are dependent on endosomal cycling and proteasome activity (53). The involvement of PID and PID-like kinases in these processes clearly requires further study.

PID possibly modulates auxin responses during embryogenesis

The crucial role of the CSN in auxin-induced, SCF^{TIR1} E3 ligase-dependent proteolysis of Aux/IAA proteins is well established (13, 15, 17). Until now, however, it was not known whether CSN-associated kinases were involved in this process, even though several protein kinases have been proposed as regulators of Aux/IAA stability (5). In this chapter we do not only provide data on a possible role of PID as CSN-associated kinase, but our results also suggest that PID reduces IAA12/BDL activity by phosphorylation of this labile transcriptional repressor close to its SCF^{TIR1}-interacting domain II (3, 61, 62). The double mutant analysis and transient protoplast expression experiments provide important *in vivo* indications for a role of PID as negative regulator of BDL activity during embryogenesis.

It remains to be determined however, whether PID-mediated BDL inhibition is due to protein degradation. In fact, the more severe *pid-bdl* phenotypes can not easily be explained in terms of reduced *iaa12/bdl* degradation, since the gain-of-function mutations in Aux/IAA proteins have been shown to disrupt the interaction with SCF^{TIR1}, thereby preventing their subsequent proteolysis (61). In the embryo, however, IAA12/BDL is known to act redundantly with IAA13 to regulate MONOPTEROS (MP)/ARF5, and possibly also NONPHOTOTROPIC HYPOCOTYL 4 (NPH4)/ARF7, -dependent embryonic organ formation (51, 63). Since IAA13, like BDL, has the PRXS motif in domain II, PID phosphorylation at this position could lead to reduced IAA13 stability. Conversely, in the *pid-bdl* double mutant, IAA13 stability would be increased, leading to a greater reduction in auxin responsive gene expression. Alternatively, PID-mediated phosphorylation could negatively interfere with the interaction between IAA12/BDL or IAA13 and ARF5/MP or ARF7/NPH4 (51, 63), thereby weakening IAA12/IAA13-mediated repression of auxin responsive genes. In this case, the moderate defects observed in *bdl* mutants could be due to the presence of PID-mediated repression of BDL/IAA13 interaction with ARF5/ARF7. In *pid-bdl* double mutants, on the other hand, absence of PID could result in enhanced repression of ARF5 or ARF7 by BDL and IAA13, thereby causing the more severe phenotypes observed in these plants.

Although the first hypothesis implies that PID phosphorylation is necessary for efficient SCF-dependent recruitment of BDL and IAA13 for proteolysis, it has been recently reported that IAA7 does not require phosphorylation in order to be degraded (10). By contrast, IAA7 does not have the PRXS motif in domain II. In fact, this motif is specific for IAA12 and IAA13, and it could very well be that the possible role of PID as modulator of auxin responses is specific for these two Aux/IAA proteins. PID is encoded by an auxin responsive gene, and as a regulator of auxin responsive gene expression it may provide a strong positive feedback on its own expression. In context to embryogenesis this may be important in allowing proper cotyledon primordia development.
A functional interaction between PID, BDL and IAA13 requires that the spatio-temporal expression of the corresponding genes overlap and that the proteins co-localize to the same subcellular compartments. Detailed expression analysis and subcellular localization studies will be important steps in future research, but currently we are testing the expression of a mutant BDL version that lacks the putative PID phosphorylation site, under control of its own promoter.

ACKNOWLEDGEMENTS

This work was financially supported by CAPES (Brazilian Federal Agency for Post-Graduate Education, M.K.-Z.). We thank Dolf Weijers for providing the plasmid pET16H-BDL, Carlos Galvan for the plasmid pET16H-PID and for the pictures of wild type and *35S::PID* seedlings, Helene Robert for the plasmid pEF-PID-FLAG, Johan Memelink for plasmid pET16H, Adam Vivian-Smith for helpful comments on the manuscript, and Peter Hock for the art work.

REFERENCE LIST

1. Liscum, E. & Reed, J. W. (2002) *Plant Mol. Biol.* **49**, 387-400.

2. Tiwari, S. B., Hagen, G. & Guilfoyle, T. J. (2004) *Plant Cell* **16**, 533-543.

3. Ramos, J. A., Zenser, N., Leyser, O. & Callis, J. (2001) *Plant Cell* **13**, 2349-2360.

4. Ulmasov, T., Hagen, G. & Guilfoyle, T. J. (1999) *Plant J.* **19**, 309-319.

5. Reed, J. W. (2001) *TRENDS in Plant Science* **Vol.6**, 420-425.

6. Hamann, T., Mayer, U. & Jurgens, G. (1999) *Development* **126**, 1387-1395.

7. Hellmann, H., Hobbie, L., Chapman, A., Dharmasiri, S., Dharmasiri, N., del Pozo, C., Reinhardt, D. & Estelle, M. (2003) *EMBO J.* **22**, 3314-3325.

8. Gray, W. M., del Pozo, J. C., Walker, L., Hobbie, L., Risseeuw, E., Banks, T., Crosby, W. L., Yang, M., Ma, H. & Estelle, M. (1999) *Genes Dev.* **13**, 1678-1691.

9. Gray, W. M., Hellmann, H., Dharmasiri, S. & Estelle, M. (2002) *Plant Cell* **14**, 2137-2144.

10. Dharmasiri, N., Dharmasiri, S. & Estelle, M. (2005) *Nature* **435**, 441-445.

11. Kepinski, S. & Leyser, O. (2005) *Nature* **435**, 446-451.

12. Pozo, J. C., Timpte, C., Tan, S., Callis, J. & Estelle, M. (1998) *Science* **280**, 1760-1763.

13. Lyapina, S., Cope, G., Shevchenko, A., Serino, G., Tsuge, T., Zhou, C., Wolf, D. A., Wei, N., Shevchenko, A. & Deshaies, R. J. (2001) *Science* **292**, 1382-1385.

14. Castle, L. A. & Meinke, D. W. (1994) *Plant Cell* **6**, 25-41.

15. Schwechheimer, C., Serino, G., Callis, J., Crosby, W. L., Lyapina, S., Deshaies, R. J., Gray, W. M., Estelle, M. & Deng, X. W. (2001) *Science* **292**, 1379-1382.

16. Bostick, M., Lochhead, S. R., Honda, A., Palmer, S. & Callis, J. (2004) *Plant Cell* **16**, 2418-2432.

17. Tao, L. Z., Cheung, A. Y., Nibau, C. & Wu, H. M. (2005) *Plant Cell* **17**, 2369-2383.

18. Friml, J., Vieten, A., Sauer, M., Weijers, D., Schwarz, H., Hamann, T., Offringa, R. & Jurgens, G. (2003) *Nature* **426**, 147-153.

19. Sabatini, S., Beis, D., Wolkenfelt, H., Murfett, J., Guilfoyle, T., Malamy, J., Benfey, P., Leyser, O., Bechtold, N., Weisbeek, P. *et al.* (1999) *Cell* **99**, 463-472.

20. Reinhardt, D., Pesce, E. R., Stieger, P., Mandel, T., Baltensperger, K., Bennett, M., Traas, J., Friml, J. & Kuhlemeier, C. (2003) *Nature* **426**, 255-260.

21. Muller, A., Guan, C., Galweiler, L., Tanzler, P., Huijser, P., Marchant, A., Parry, G., Bennett, M., Wisman, E. & Palme, K. (1998) *EMBO J.* **17**, 6903-6911.

22. Friml, J., Wisniewska, J., Benkova, E., Mendgen, K. & Palme, K. (2002) *Nature* **415**, 806-809.

23. Luschnig, C., Gaxiola, R. A., Grisafi, P. & Fink, G. R. (1998) *Genes Dev.* **12**, 2175-2187.

24. Raven, J. (1975) *New Phytologist* **74**, 163-172.

25. Rubery, P. H. & Sheldrake, A. R. (1974) *Planta* **118**, 101-121.

26. Okada, K., Ueda, J., Komaki, M. K., Bell, C. J. & Shimura, Y. (1991) *Plant Cell* **3**, 677-684.

27. Galweiler, L., Guan, C., Muller, A., Wisman, E., Mendgen, K., Yephremov, A. & Palme, K. (1998) *Science* **282**, 2226-2230.

28. Friml, J., Benkova, E., Blilou, I., Wisniewska, J., Hamann, T., Ljung, K., Woody, S., Sandberg, G., Scheres, B., Jurgens, G. *et al.* (2002) *Cell* **108**, 661-673.

29. Petrasek, J., Mravec, J., Bouchard, R., Blakeslee, J. J., Abas, M., Seifertova, D., Wisniewska, J., Tadele, Z., Kubes, M., Covanova, M. *et al.* (2006) *Science*.

30. Wisniewska, J., Xu, J., Seifertova, D., Brewer, P. B., Ruzicka, K., Blilou, I., Roquie, D., Benkova, E., Scheres, B. & Friml, J. (2006) *Science*.

31. Chen, R., Hilson, P., Sedbrook, J., Rosen, E., Caspar, T. & Masson, P. H. (1998) *Proc Natl. Acad. Sci. U S. A* **95**, 15112-15117.

32. Friml, J., Yang, X., Michniewicz, M., Weijers, D., Quint, A., Tietz, O., Benjamins, R., Ouwerkerk, P. B., Ljung, K., Sandberg, G. *et al.* (2004) *Science* **306**, 862-865.

33. Benjamins, R., Quint, A., Weijers, D., Hooykaas, P. & Offringa, R. (2001) *Development* **128**, 4057-4067.

34. Serino, G., Su, H., Peng, Z., Tsuge, T., Wei, N., Gu, H. & Deng, X. W. (2003) *The Plant Cell* **15**, 719–731.

35. Sambrook, J., Fritsch, F. & Maniatis, T. (1989) *Molecular Cloning - A Laboratory Manual* (Cold Spring Habour Laboratory Press, New York).

36. Benjamins, R. Functional analysis of the PINOID protein kinase in *Arabidopsis thaliana*. 2004. Leiden University.

37. Benjamins, R., Ampudia, C. S., Hooykaas, P. J. & Offringa, R. (2003) *Plant Physiol* **132**, 1623-1630.

38. Schirawski, J., Planchais, S. & Haenni, A. L. (2000) *J Virol. Methods* **86**, 85-94.

39. Axelos, M., Curie, C., Mazzolini, L., Bardet, C. & Lescure, B. (1992) *Plant Physiol Biochem* **30**, 123-128.

40. Masson, J. & Paszkowski, J. (1992) *Plant J* **2**, 208-218.

41. Uhle, S., Medalia, O., Waldron, R., Dumdey, R., Henklein, P., Bech-Otschir, D., Huang, X., Berse, M., Sperling, J., Schade, R. *et al.* (2003) *EMBO J.* **22**, 1302-1312.

42. Bech-Otschir, D., Seeger, M. & Dubiel, W. (2002) *J. Cell Sci.* **115**, 467-473.

43. Blom, N., Gammeltoft, S. & Brunak, S. (1999) *J Mol Biol* **294**, 1351-1362.

44. Gattiker, A., Gasteiger, E. & Bairoch, A. (2002) *Appl. Bioinformatics.* **1**, 107-108.

45. Schwechheimer, C. (2004) *Biochim. Biophys. Acta* **1695**, 45-54.

46. Bennett, S., Alvarez, J., Bossinger, G. & Smyth, D. (1995) *Plant J.* **8** , 505.

47. Christensen, S. K., Dagenais, N., Chory, J. & Weigel, D. (2000) *Cell* **100**, 469-478.

48. Chamovitz, D. A., Wei, N., Osterlund, M. T., von Arnim, A. G., Staub, J. M., Matsui, M. & Deng, X. W. (1996) *Cell* **86**, 115-121.

49. Furutani, M., Vernoux, T., Traas, J., Kato, T., Tasaka, M. & Aida, M. (2004) *Development* **131**, 5021-5030.

50. Torres-Ruiz, R. A., Lohner, A. & Jurgens, G. (1996) *Plant J.* **10**, 1005-1016.

51. Weijers, D., Benkova, E., Jager, K. E., Schlereth, A., Hamann, T., Kientz, M., Wilmoth, J. C., Reed, J. W. & Jurgens, G. (2005) *EMBO J.* **24**, 1874-1885.

52. Paciorek, T., Zazimalova, E., Ruthardt, N., Petrasek, J., Stierhof, Y. D., Kleine-Vehn, J., Morris, D. A., Emans, N., Jurgens, G., Geldner, N. *et al.* (2005) *Nature* **435**, 1251-1256.

53. Abas, L., Benjamins, R., Malenica, N., Paciorek, T., Wirniewska, J., Moulinier-Anzola, J. C., Sieberer, T., Friml, J. & Luschnig, C. (2006) *Nat. Cell Biol.* **8**, 249-256.

54. Sun, Y., Wilson, M. P. & Majerus, P. W. (2002) *J. Biol. Chem.* **277**, 45759-45764.

55. Seeger, M., Kraft, R., Ferrell, K., Bech-Otschir, D., Dumdey, R., Schade, R., Gordon, C., Naumann, M. & Dubiel, W. (1998) *FASEB J* **12**, 469-478.

56. Wilson, M. P., Sun, Y., Cao, L. & Majerus, P. W. (2001) *J. Biol. Chem.* **276**, 40998-41004.

57. Ang, L. H., Chattopadhyay, S., Wei, N., Oyama, T., Okada, K., Batschauer, A. & Deng, X. W. (1998) *Mol. Cell* **1**, 213-222.

58. Hardtke, C. S., Gohda, K., Osterlund, M. T., Oyama, T., Okada, K. & Deng, X. W. (2000) *EMBO J.* **19**, 4997-5006.

59. Lee, Y., Lloyd, A. M. & Roux, S. J. (1999) *Plant Physiol* **119**, 989-1000.

60. Bonifacino, J. S. & Traub, L. M. (2003) *Annu. Rev. Biochem* **72**, 395-447.

61. Gray, W. M., Kepinski, S., Rouse, D., Leyser, O. & Estelle, M. (2001) *Nature* **414**, 271-276.

62. Kepinski, S. & Leyser, O. (2002) *Plant Cell* **14 Suppl**, S81-S95.

63. Hardtke, C. S., Ckurshumova, W., Vidaurre, D. P., Singh, S. A., Stamatiou, G., Tiwari, S. B., Hagen, G., Guilfoyle, T. J. & Berleth, T. (2004) *Development* **131**, 1089-1100.